RMetS
Royal Meteorological Society

The role of cold fronts in the onset of the monsoon season in the South Atlantic convergence zone

Rosana Nieto-Ferreira,* Thomas M. Rickenbach and Emily A. Wright
Department of Geography, East Carolina University, Greenville, North Carolina, USA
*Correspondence to: R. Nieto-Ferreira, East Carolina University Geography, A-227 Brewster Building, Greenville, North Carolina 27858-4353, USA. E-mail: ferreirar@ecu.edu

The onset of the South American monsoon season culminates with the abrupt establishment of the South American convergence zone (SACZ). The impact of cold fronts on the abrupt establishment of the SACZ is studied using an 11-year composite analysis of the dynamic and thermodynamic structures, intensity and propagation of cold fronts that occur prior to, during, and after monsoon onset in the SACZ. A significant change in the structure and propagation of cold fronts is observed at the time of monsoon onset in the SACZ, with cold fronts suddenly stalling and becoming stationary in southeastern Brazil. It is proposed that this regime change of the structure and propagation of cold fronts causes the abrupt onset of the monsoon in the SACZ. A mechanism for this sudden change in cold front behaviour is suggested by analyzing changes in the observed upper-level structure of midlatitude waves. Our observations show that, at the time of monsoon onset in the SACZ, midlatitude waves develop a 'thinning trough' behaviour, with upper-level troughs becoming thinner, westward tilted, and sometimes forming cut-off lows. This behaviour is characteristic of midlatitude waves that develop in the region of anticyclonic shear on the equatorward side of the upper-level midlatitude jet. During the austral spring, the upper-level midlatitude jet over South America migrates southward leaving subtropical South America in the equatorward, anticyclonic shear side of the jet. It is hypothesized that, as the meridional shear on the equatorward side of the upper-level jet gradually becomes more anticyclonic, it suddenly crosses the critical threshold of horizontal shear that has been shown to produce a sudden transition to a 'thinning trough' midlatitude wave regime. At this time a regime change occurs whereby the character of frontal systems crossing South America changes abruptly, causing the onset of the monsoon season in the SACZ.

Key Words: SACZ; midlatitude cyclones; thinning troughs; onset; cold fronts

Received 2 March 2010; Revised 19 December 2010; Accepted 22 February 2011; Published online in Wiley Online Library 16 May 2011

Citation: Nieto-Ferreira R, Rickenbach TM, Wright EA. 2011. The role of cold fronts in the onset of the monsoon season in the South Atlantic convergence zone. *Q. J. R. Meteorol. Soc.* **137**: 908–922. DOI:10.1002/qj.810

1. Introduction

The seasonal cycle of precipitation in tropical South America shares general characteristics with classical monsoon climates in other parts of the world (Zhou and Lau, 1998) and is therefore referred to as the South American Monsoon System (SAMS). The evolution of monsoon onset across South America has complex temporal and regional variability (Kousky, 1988; Horel *et al.*, 1989; Marengo *et al.*, 2001; Liebmann and Marengo, 2001; Li and Fu, 2004) that

are controlled by local and remote land–ocean–atmosphere processes. Nieto-Ferreira and Rickenbach (2011, henceforth NR11) combined results from a rainfall threshold analysis and a rotated empirical orthogonal function (REOF) analysis of the Global Precipitation Climatology Project version 2 pentad dataset (GPCPv2) to propose a three-stage conceptual model for SAMS onset. In this model, stage 1 of monsoon onset begins around pentad 58 (13 to 17 October) when precipitation starts in the northwestern part of South America and then gradually progresses south and southeastward. Stage 2 of monsoon onset is marked by the abrupt onset of the South Atlantic convergence zone (SACZ), identified as a southeastward extension of cloudiness from the continent into the Atlantic Ocean, around pentad 61 (28 October and 1 November). Stage 3 of SAMS onset involves the late arrival of the monsoon to the mouth of the Amazon River, associated with the slow migration of the Atlantic intertropical convergence zone. This final stage of onset occurs on average by pentad 73 (27 to 31 December).

This three-stage model of SAMS onset provides a useful framework for the study of regional differences in monsoon onset mechanisms. The gradual onset of the monsoon season in the Amazon basin is likely driven by the thermodynamic priming (or gradual build-up of convective available potential energy) of the atmosphere, which is in turn driven by the southward migration of the sun (Fu and Li, 2004; Li and Fu, 2004). On the other hand, the abrupt onset of the monsoon season in the SACZ region is very likely dynamically driven. A possible mechanism to explain the abrupt onset of the monsoon season in the SACZ are the fast dynamic and thermodynamic changes caused by the passage of cold front systems (Li and Fu, 2006; Gonzalez *et al.*, 2007; Raia and Cavalcanti, 2008). Over South America, cold fronts can move far northward and influence precipitation in the Tropics and Subtropics (Fortune and Kousky, 1983; Garreaud, 2000; Vera and Vigliarolo, 2000). Li and Fu (2006) suggested that cold air surges – or strong cold front events – participate in SAMS onset through enhancement of forced ascent in a thermodynamically primed atmosphere. Frontal systems have also been recognized to play an important role in monsoon onset over the South China Sea (Chang and Chen, 1995) as warm moist southwesterly flow produces widespread rain along cold fronts that become stationary (termed the Baiyu or Mei-yu front). This study addresses the role of frontal systems in triggering the abrupt onset of the SACZ.

The SACZ is the hallmark feature of the mature SAMS and is easily identified in time-averaged maps of austral summer rainfall as a distinctive northwest–southeast oriented band of rainfall that connects the western Amazon basin and the South Atlantic Ocean. The SACZ can be thought of as a time-averaged manifestation of stationary frontal zones. On submonthly time-scales, each SACZ episode is composed of one or more cold front systems that intrude into the Tropics and Subtropics and become stationary for a few days over southeastern Brazil. Once established, the SACZ has strong variability on intraseasonal time-scales (e.g. Liebmann *et al.*, 1999; Nieto-Ferreira *et al.*, 2003) and modulates the amount and organization of rainfall well into the western Amazon basin (Rickenbach *et al.*, 2002).

The term 'cold surge' is generally used to denote strong cold frontal passages through South America (e.g. Fortune and Kousky, 1983; Garreaud, 2000; Marengo *et al.*, 1997). Previous studies have attributed the occurrence of 'cold surges' to the impact of the Andes Mountains on eastward propagating synoptic-scale transient disturbances (Garreaud, 2000; Lupo *et al.*, 2001). During a 'cold surge' event, cold air damming enhances the northward flow of cold air along the eastern side of the Andes Mountains. On the leading edge of a surface anticyclone that is crossing over the Andes from the Eastern Pacific into South America, cold air damming produces a strong southerly barrier jet along the eastern side of the Andes and a strong northward cold air advection into subtropical and tropical South America (e.g. Garreaud, 2000; Lupo *et al.*, 2001). Those studies also show that the anticyclone on the eastern side of the Andes displays the marked meridional elongation and anticyclonic trajectory turning that are the trademark influences of mountains on transient disturbances (Gan and Rao, 1984). The Andes therefore help promote the incursion of midlatitude cold fronts and cold midlatitude air well into the Subtropics and Tropics of South America, a phenomenon that is commonly observed to the east of major north–south oriented mountain ranges (Lupo *et al.*, 2001).

Garreaud (2000) used the steep rise in sea-level pressure (SLP) at the leading edge of the anticyclone associated with a cold front to identify the passage of cold surges through South America. Using this definition, they found an average of nine cold surge episodes per year during May–September and eight cold surge episodes per year during November–March. That study showed that cold fronts undergo a seasonal transition in structure, intensity and propagation. Composite fields for the day of the cold surge event and the two days preceding and following the event showed significant differences between the evolution of summertime and wintertime cold surge events. Wintertime events bring very strong negative temperature anomalies to southern South America accompanied by a weak band of convective cloudiness that affects coastal regions of southern Brazil. On the other hand, summertime events bring very weak temperature anomalies but organize a northwest–southeast oriented band of convection that stretches from western Amazonia through southeastern Brazil and into the South Atlantic Ocean, in a way that is similar to the observed structure of the SACZ.

Warm and cold frontal systems are the surface signature of midlatitude cyclones. The aforementioned seasonal transition in the structure, intensity and propagation of cold fronts over South America may therefore be caused by changes in the structure, propagation, or intensity of their 'parent' midlatitude cyclones. Modelling studies have in fact shown that the structure and propagation of frontal systems are controlled by the behaviour of their 'parent' midlatitude cyclone, which is in turn largely determined by the direction and strength of the tropospheric horizontal shear. Whereas the atmosphere exhibits a wide range of midlatitude cyclone behaviour, numerical modelling studies have shown that even modest changes in environmental shear can produce dramatically different midlatitude cyclone morphologies that affect not only the upper-level features of a midlatitude cyclone but also the strength, propagation, and length of its surface warm and cold fronts (e.g. Hoskins and West, 1979; Davies *et al.*, 1991; Thorncroft *et al.*, 1993). Midlatitude cyclones that are embedded in an environment with stronger cyclonic shear, also known as 'cyclonic behaviour', tend to form upper level 'broadening troughs', weaker surface cold fronts, and strong warm fronts. On

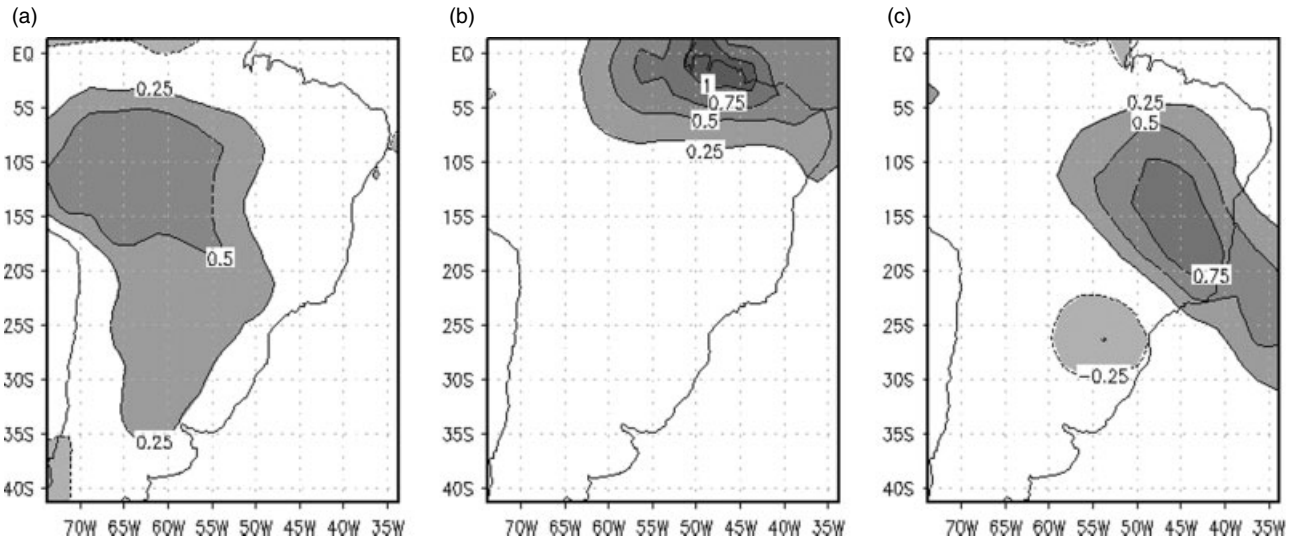

Figure 1. First three rotated empirical orthogonal functions (REOFs) of the GPCP pentad data from 1979 to 2008. (a) REOF 1 (14%), (b) REOF 2 (12%) and (c) REOF 3 (11%).

the other hand, when midlatitude cyclones form in an environment characterized by stronger anticyclonic shear they tend to evolve into upper-level 'thinning troughs' that become tilted westward as they advance into lower latitudes, sometimes producing cut-off cyclones. These so-called 'anticyclonic behaviour' midlatitude cyclones tend to produce strong, elongated, slower-moving surface cold fronts and little or no warm front signature. Shapiro *et al.* (2001) studied the effect of El Niño on the frequency of occurrence of 'anticyclonic' *versus* 'cyclonic' midlatitude cyclone behaviour in the Eastern Pacific and western North America. Their results suggest that the changes in environmental shear that occur in the Eastern Pacific and western North America during El Niño and La Niña years modulate the type of baroclinic wave life cycle. During the 1998–1999 La Niña event, the upper-level jet was weakened and displaced northward producing anticyclonic shear in the latitude belt where midlatitude waves propagate and causing more thinning trough or 'anticyclonic behaviour' days. During the 1997–1998 El Niño, the midlatitude jet was stronger and displaced southward so that 'cyclonic' shear was present and more 'broadening trough' or 'cyclonic behaviour' events were observed. Incidentally they find that 'anticyclonic' or 'thinning trough' events had lower predictability than their cyclonic counterparts.

In this study, composites of cold fronts that occurred prior to and during monsoon onset in the SACZ region are compared to analyse the role of cold fronts on the onset of the SAMS. Section 2 introduces the datasets used in this study. The dates of cold front passage through South America and monsoon onset date in the SACZ are determined in section 3. Section 4 presents an analysis of composite maps of the structure and temporal evolution of cold fronts prior to and during monsoon onset in the SACZ region. Section 5 suggests a possible dynamical trigger for the abrupt onset of the monsoon season in the SACZ. Conclusions and suggestions for future work are presented in section 6.

2. Datasets

The precipitation dataset chosen for this study is the Global Precipitation Climatology Project (GPCP) dataset (Adler

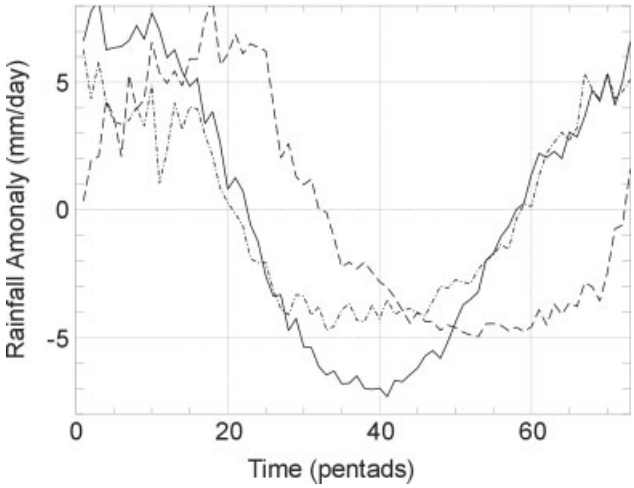

Figure 2. Annual mean time series of the first three PCs of the 1979–2008 GPCP pentad rainfall REOF analysis (PC1 solid, PC2 dashed, PC3 dot-dashed).

et al., 2003). The strength of the GPCP rainfall products is that they are uniform in time and space, cover all of South America, and are tuned to the more physically direct precipitation retrievals of microwave satellites. In addition the GPCP datasets are calibrated with surface rain gauges, and are subject to stringent quality control (Adler *et al.*, 2003). Two versions of this dataset are used in this study. The GPCPv2.1 dataset (1979–present) consists of pentads (5-day averaged) of 2.5° resolution precipitation data. Although the GPCP one-degree daily (1dd) dataset (Huffman *et al.*, 2001) is available only since late 1997, its higher horizontal (1°) and temporal (1 day) resolutions make it more appropriate than the GPCPv2 data for studying phenomena such as cold fronts that vary on sub-pentad time-scales. The GPCP1dd is therefore used in this study to produce cold front composites in and around the time of monsoon onset in the SACZ region.

The National Center for Environmental Prediction (NCEP) reanalysis (Kalnay *et al.*, 1996) dataset is used to determine not only the dates when cold fronts

Table I. Onset pentads and corresponding calendar dates, plus dates (in Julian days) of the last 'pre-onset' cold front, the 'onset' cold front and the first 'post-onset' cold front for the period 1998–2008.

Year	Onset pentad	Onset date	Pre-onset cold front	Onset cold front	Post-onset cold front
1998	61	28 Oct–1 Nov	291	297	322
1999	59	18–22 Oct	281	291	297
2000	61	28 Oct–1 Nov	298	301	319
2001	59	18–22 Oct	282	289	295
2002	61	28 Oct–1 Nov	294	303	308
2003	62	2–6 Nov	300	305	317
2004	64	12–16 Nov	316	322	361
2005	61	28 Oct–1 Nov	290	302	310
2006	58	13–17 Oct	279	289	293
2007	66	22–26 Nov	319	324	330
2008	61	28 Oct–1 Nov	308	314	321

occurred but also to characterize the changes in synoptic-scale flow fields associated with the passage of cold fronts through South America prior to, during, and shortly after monsoon onset. Daily averages of the NCEP reanalysis sea-level pressure, temperature, geopotential height and wind fields at a 2.5° horizontal resolution were used.

3. Cold fronts and SACZ onset dates

The NCEP/NCAR reanalysis SLP was used to determine the dates of all cold fronts that occurred during 1979–2008. The Garreaud (2000) definition of a cold surge – or strong cold front – was used as a starting point for defining cold fronts in this study. Garreaud (2000) defined a cold surge as the days that fell in the top 10% of the seasonal frequency distribution of the 24-hour SLP tendency in the $5^\circ \times 5^\circ$ box centred at 27°S, 57.5°W. To ensure that the strong SLP tendencies were associated with a strong cold front, Garreaud (2000) furthermore required that SLP $\geqslant$1020 mb, indicating the presence of a strong anticyclone. In this study the definition of cold surge used in Garreaud (2000) was relaxed to allow detection of most cold fronts – not just strong events – that passed through South America over the year. For this study a cold front is catalogued on days when the 24-hour SLP tendency in the $5^\circ \times 5^\circ$ box centred at 23.75°S, 58.75°W (hereafter referred to as the *base region*) exceeded 1.5 mb for SLP higher than 1005 mb. Cold front events that persisted for several days were only counted once. Using this definition, a total of 1764 cold front episodes were catalogued during 1979–2008. On average, five cold front episodes occurred each month, so that on average about one cold front per week crossed the base region. A weak annual cycle is present with a minimum of 4.2 cold fronts per month in February and a maximum of 5.6 cold fronts in July.

NR11 performed an REOF analysis of the 1979–2008 GPCPv2.1 pentad dataset at 2.5° horizontal resolution over the domain indicated in Figure 1 to study the main modes of spatial and temporal variability over South America. The principal component (PC) for each REOF captures variability on time-scales from 5 days to interannual, including intraseasonal variability and the seasonal cycle. Three distinct modes* of variability were captured by this REOF analysis (Figure 1). The first and second REOFs represent the variability of rainfall in the western two-thirds of the Amazon basin and in the northeastern SAMS between 0 and 10°S, respectively. This study focuses on the variability of rainfall in the SACZ region which in this analysis is captured by the third REOF (REOF3; Figure 1(c)). REOF3 exhibits a dipole pattern of rainfall variability with a weaker centre in southern Brazil and Uruguay and a stronger centre of opposite sign anomalies extending southeastward from southeastern Brazil into the Atlantic Ocean. This dipole pattern represents variability associated with the SACZ and explains about 11% of the variance. Nogues-Paegle and Mo (1997) filtered outgoing long-wave radiation to show that a very similar dipole pattern occurs in intraseasonal time-scales from 10 to 90 days.

Figure 2 shows the 30-year averaged principal component (PC3) time series annual cycle for each of the first three REOF patterns. The PC3 time series (Figure 2) captures the annual cycle of rainfall variability over the SACZ and was used by NR10 to define the climatological date of onset of the SACZ as the time when rainfall anomalies given by the PC3 time series become positive. According to this criterion, the SACZ region monsoon season begins on average at around pentad 61 (28 October–1 November) with a standard deviation of 3.7 pentads. The monsoon retreats in the SACZ region by the following April (pentad 21) when the rainfall maximum returns to the southern side of the dipole located over southern Brazil. Applying the same criterion to the PC1 time series, NR10 determined that the onset date for the Amazon basin occurs on average on pentad 58 (13–17 October) with a standard deviation of 2.1 pentads. This means that on average the SACZ becomes established after monsoon onset occurs in the Amazon basin, suggesting that the onset of the monsoon over the Amazon basin may help set the stage for the establishment of the SACZ, as will be discussed in the next section. This connection stems also from moisture convergence in the low-level northwesterly jet that transports water vapour from the Amazon basin to the SACZ during the monsoon season (Rickenbach *et al.*, 2002). The interannual variability of onset dates (measured by the standard deviation of the onset dates) is larger in

*According to the rule of thumb established by North *et al.* (1982).

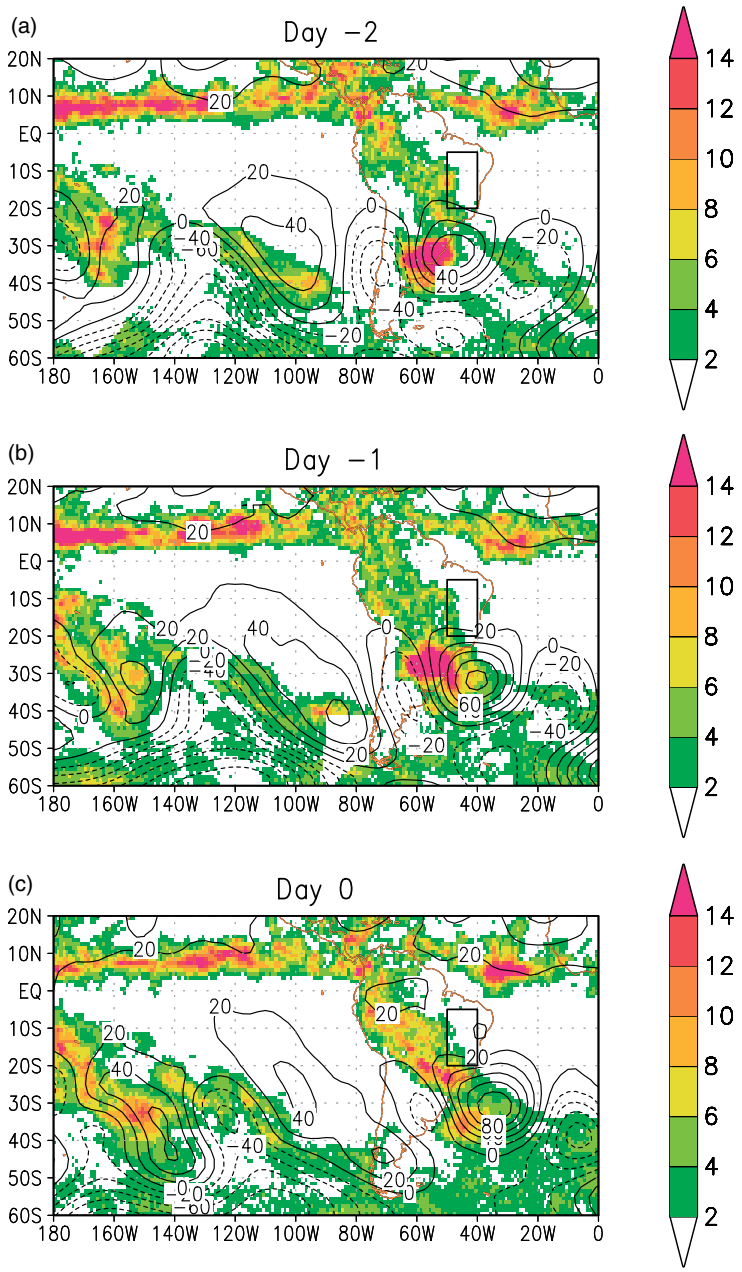

Figure 3. 'Pre-onset' cold front composites of daily 200 mb geopotential height anomalies (contours, m) from the October to November 1998–2008 mean and daily GPCP rainfall (shading, mm day^{-1}) for 1998–2008. Daily composite plots are shown from (a) two days before (day −2) to (f) three days after (day +3) cold front passage through the base region. The solid box indicates the SACZ region. This figure is available in colour online at wileyonlinelibrary.com/journal/qj

the SACZ than in the Amazon basin, also pointing to the possible role of a more stochastic mechanism, such as the variability associated with cold fronts, in monsoon onset.

In this study, the REOF analysis of the GPCP rainfall pentads was used to determine the date of onset of the SACZ for each year between 1998 and 2008 in a way that is similar to NR11. For each year, SACZ onset was defined as the pentad when the PC time series for REOF3 becomes positive and remains positive during the next pentad and for at least six of the next eight pentads. The dates of monsoon onset in the SACZ region for each year are shown in Table I. In agreement with the longer time series, the average onset date for this period is pentad 61 (28 October–1 November) with the earliest onset of the study period occurring in 2006 (pentad 58, 13–17 October) and the latest onset occurring in 2007 (pentad 66, 22–26 November).

Monsoon onset pentad dates in the SACZ region were then used to select for each year the last cold front that preceded onset ('pre-onset'), the cold front that occurred during the onset pentad ('onset'), and the first cold front following onset ('post-onset'). The dates of pre-onset, onset, and post-onset cold fronts are also shown in Table I.

4. 'Pre-Onset' and 'Onset' cold front composites

Figures 3 and 4 show the 11-year composites of GPCP rainfall and 200 mb geopotential height anomalies for the pre-onset and onset cold front systems, respectively. Geopotential height anomalies are calculated based on the October to November 1998–2008 mean. Post-onset composites are not

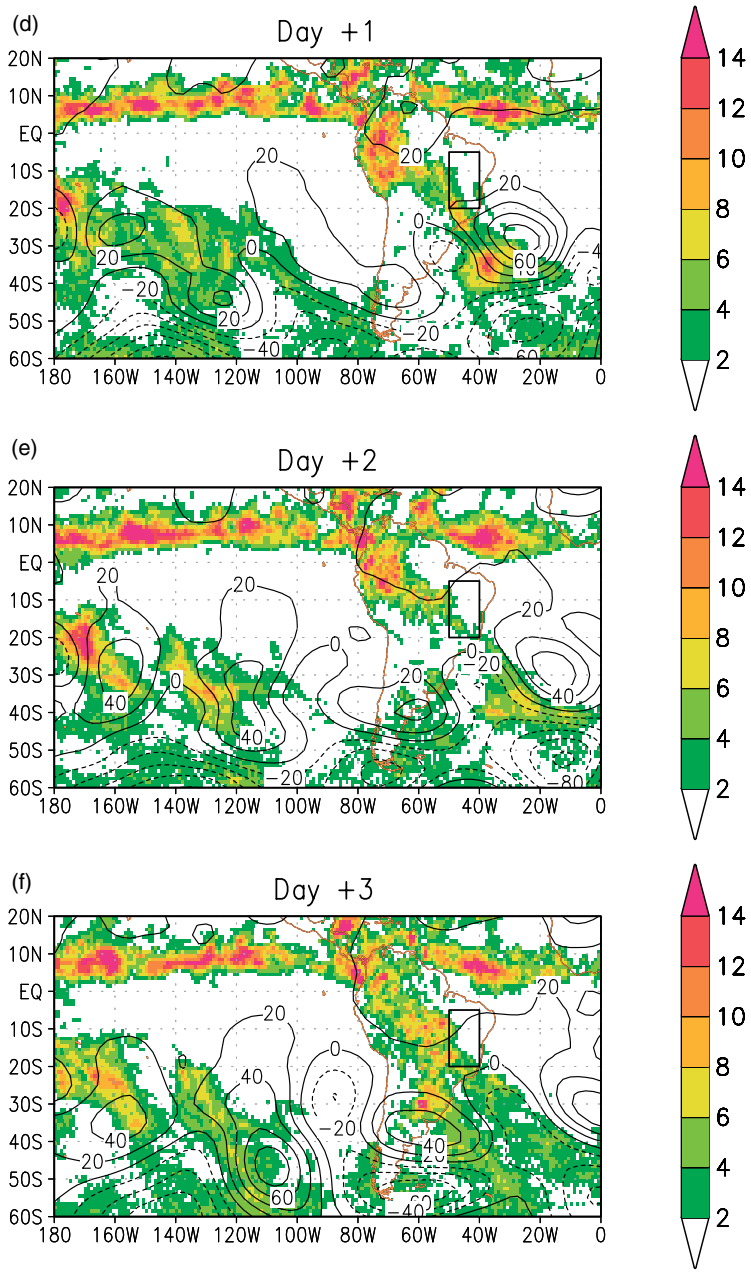

Figure 3. (*continued*) This figure is available in colour online at wileyonlinelibrary.com/journal/qj

shown because they are very similar to the onset composites. The composites are shown on the day the cold front is defined (day 0) as well as on the nth day prior to the cold front passage (day$-n$) and on the nth day after the cold front passage (day$+n$). Although only 11 cases are included in each composite, the temporal and spatial structure coherence of the composites suggests that enough cold front events were included in each composite to extract the signal of frontal passages through South America at pre-onset and onset.

In both composites, rainfall is already present over the western two-thirds of the Amazon basin prior to the passage of the cold fronts, consistent with the observation (NR10) that onset in the western two-thirds of the Amazon basin precedes onset in the SACZ. On day -2 and day -1 the pre-onset composite (Figure 3(a,b)) has somewhat weaker precipitation in the Amazon basin than the onset composite (Figure 4(a,b)). During that time the pre-onset composite has very large and strong rainfall maxima in Uruguay and southern Brazil, indicating the presence of mesoscale convective complexes (Velasco and Fritsch, 1987) just before the cold front passes through the base region on day 0. In both composites the cold fronts propagate northeastward along the coast of South America during day -2 and day -1, reaching the coast of São Paulo and Rio de Janeiro states (Brazil) on day 0 (Figures 3(c) and 4(c)). At this time both composites show an elongated region of enhanced rainfall that stretches northwestward from the southeastern coast of Brazil all the way to the Amazon basin. During day -2 to day 0, the evolution of the rainfall associated with frontal systems in the pre-onset and onset composites is very similar. Over the western Amazon basin, convection weakens after day $+1$ in both composites (Figures 3(d) and 4(d)). However, to the east of 50°W the evolution of the pre-onset and onset cold fronts becomes dramatically different beyond day 0. After day 0, the pre-onset cold fronts weaken,

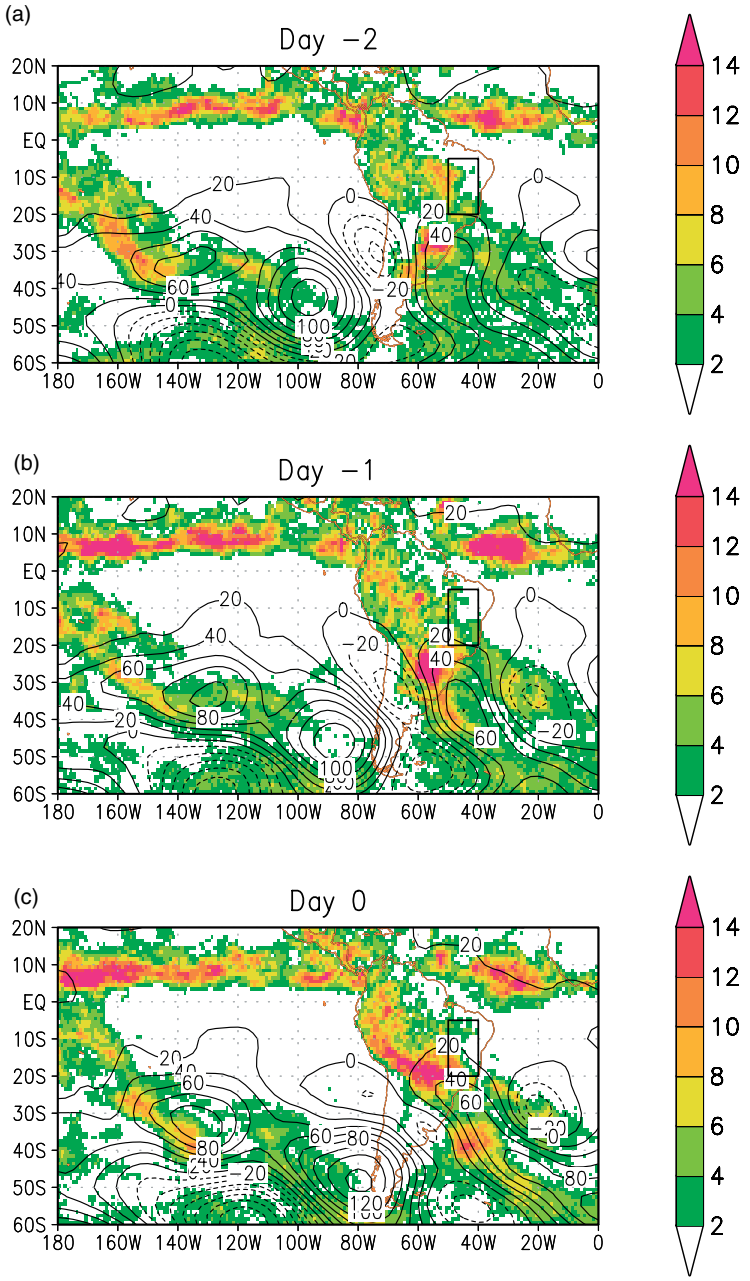

Figure 4. As Figure 3, but for the 'onset' cold front composites. This figure is available in colour online at wileyonlinelibrary.com/journal/qj

become disconnected from the Amazon basin rainfall and propagate into the South Atlantic Ocean, without ever reaching the SACZ region (Figure 3(d–f)). In contrast, the rainfall associated with the onset cold fronts continues to propagate northeastward along the South American coast becoming stationary along the SACZ region until at least day +6 (not shown), all the while configured as a northwest-to-southeast elongated region of rainfall that extends from the Amazon basin into the South Atlantic Ocean (Figure 4(c–f)). This abrupt change in the structure and propagation of frontal systems coincides with the abrupt onset of the SACZ. The abrupt onset of the SACZ therefore occurs at the time when the first cold front of the monsoon season stalls and becomes stationary along the southeastern coast of Brazil. A case-by-case visual inspection of the time series of rainfall associated with each of the onset and pre-onset cold fronts that make up the composites (not shown) shows a consistent difference between the evolution of onset and pre-onset cold fronts that supports the idea that an abrupt change occurs at the time of onset with cold fronts becoming stationary as they reach the SACZ.

The difference fields between the rainfall in the onset and pre-onset composites on day −2 to day +6 are shown in Figure 5. Values that are significant at the 90% level according to a Student *t*-test are shaded. During day −2 to day +6, no significant difference in rainfall between the onset and pre-onset composites occurs over the western two-thirds of the Amazon Basin (Figure 5). This is in good agreement with the fact that both onset and pre-onset composites show plentiful rainfall throughout the passage of cold fronts in that region (Figures 3 and 4). Prior to day 0 (Figure 5(a–c)), pre-onset and onset rainfall are not significantly different from each other in the SACZ region either, where it is dry in both composites. However, from day +1 to day +6 the onset composite has significantly more rainfall in a stationary northwest–southeast oriented band

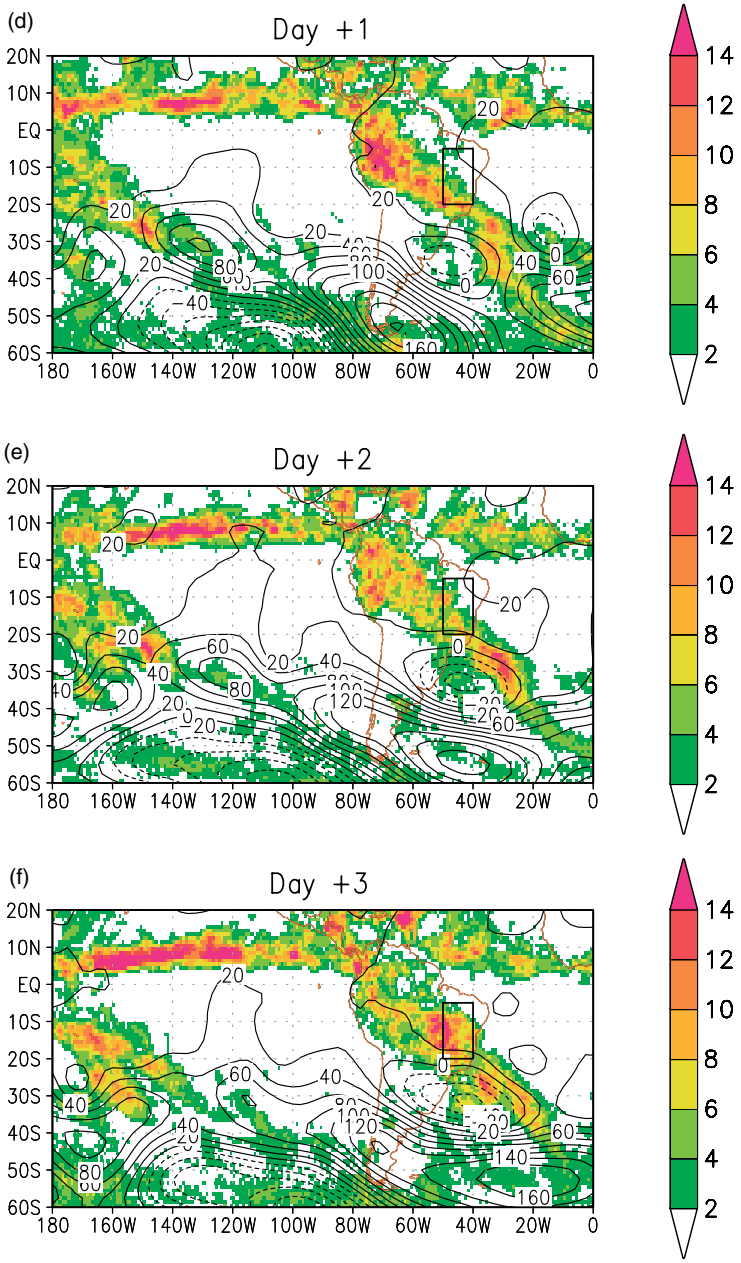

Figure 4. (*continued*) This figure is available in colour online at wileyonlinelibrary.com/journal/qj

of rainfall that crosses the SACZ region (Figure 5(d–i)). On day −2, significantly more rainfall occurs in Uruguay during pre-onset cold fronts than during onset cold fronts.

The evolution of the SLP, 925 mb air temperature, and 850 mb wind anomaly fields is very similar for the two composites between day −2 and day 0 (not shown). During that time, a high-pressure anomaly progresses northward and eastward as it crosses the Andes bringing southerly winds and strong negative temperature anomalies of up to 6°C to subtropical and parts of tropical South America. After day 0, the evolution of the low-level fields in the two composites becomes very different. The onset composite is marked by the presence of a stationary low SLP anomaly centred over the South Atlantic at 30°W and 30°S. Behind the stationary cold front there is a cold air temperature anomaly that, albeit weaker than before, occupies a large area from Bolivia to the South Atlantic and persists for a few days after day 0.

The upper-level geopotential height anomaly fields (Figures 3 and 4) may help shed some light on the question of what brings about the abrupt change in the propagation and structure of cold fronts at the time of onset in the SACZ region. Eastward migrating negative geopotential height anomalies in both composites mark the presence of an upper-level trough that approaches southern Chile from the Pacific Ocean on day −2 (Figures 3(a) and 4(a)) and continues to propagate eastward on day −1 (Figures 3(b) and 4(b)). The cold front rainfall remains ahead of the upper-level migratory trough, a region that favours the rising air and low-level convergence that are dynamically needed to sustain the rainfall along the cold front. On day −2 the pre-onset upper-level trough (Figure 3(a)) has stronger negative geopotential height anomalies than the onset upper-level trough (Figure 4(a)). By day +1, the onset upper-level trough intensifies and becomes elongated in the northwest–southeast direction as it continues to propagate eastward (Figure 4(c)). On day +2 (Figures 3(e) and 4(e))

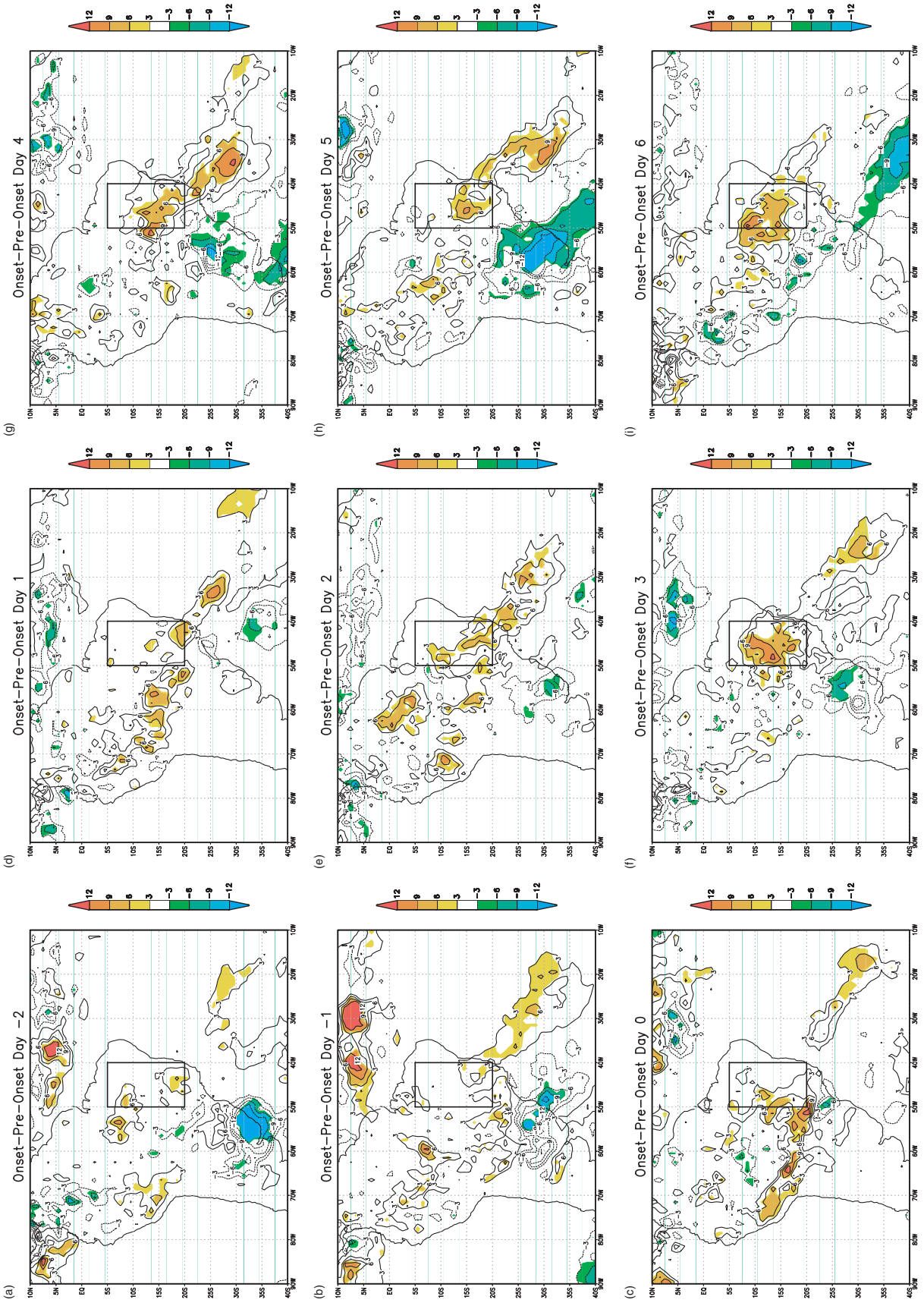

Figure 5. The difference fields (mm day^{-1}) between the rainfall in the 'onset' and 'pre-onset' composites on (a) day −2 to (i) day +6. Values that are significant at the 90% level according to a Student *t*-test are shaded. This figure is available in colour online at wileyonlinelibrary.com/journal/qj

and day +3 (Figures 3(f) and 4(f)), the upper-level negative geopotential height anomalies associated with both pre-onset and onset cold fronts are located in the South Atlantic. From day +1 to day +6 the onset upper-level negative geopotential height anomaly centre is stationary and has a distinctive zonally oriented cut-off appearance. Previous studies have in fact shown that upper-level cut-off lows are observed over South America and the nearby South Atlantic primarily during the summertime (e.g. Kousky and Gan, 1981). Between day +2 and day +6, the geopotential anomaly pattern of the onset cold front composite over South America resembles a blocking pattern (e.g. Mendes *et al.*, 2008). However, composites of rainfall associated with summertime and springtime blocking events (Mendes *et al.*, 2008) show no increase in precipitation in tropical South America associated with blocking events. Since blocking events are relatively rare in the South American sector (only four summertime events and 21 springtime events over the 41 years covered by Mendes *et al.*, 2008), it is unlikely that blocking causes monsoon onset in the SACZ or that the active phases of the SACZ are associated with blocking as suggested by Silva and Kousky (2001).

5. A possible dynamical trigger for the abrupt onset of the monsoon season in the SACZ

The analysis of the pre-onset and onset composites in section 4 suggests that changes in the propagation and structure of cold fronts are the dynamical trigger associated with the abrupt onset of the monsoon season in the SACZ region. In particular the onset composite's upper-level trough progression from a north–south, to a northwest–southeast oriented feature and finally to an east–west oriented feature (Figure 4) suggests that this trough is embedded in anticyclonic environmental horizontal shear.

It is well known that the behaviour of midlatitude cyclones and their surface cold fronts is largely determined by the direction and strength of horizontal shear (e.g. Hoskins and West, 1979; Davies *et al.*, 1991; Thorncroft *et al.*, 1993). Figure 6 shows the low-level temperature and potential temperature, θ, on the -2 PVU (potential vorticity unit $= 10^{-6}$ s^{-1} K kg^{-1}) surface on the ninth day of the 'anticyclonic' (Figure 6(a) and (b)) and 'cyclonic' (Figure 6(c) and (d)) baroclinic wave life-cycle simulations in Thorncroft *et al.* (1993), adapted here to the Southern Hemisphere. In the presence of enhanced anticyclonic environmental shear, the upper-level trough thins as it advances into subtropical latitudes and its axis rotates anticyclonically, sometimes producing upper-level cut-off lows such as the feature highlighted by the dashed box in Figure 6(b). In the subtropics, the cut-off low becomes stationary, as does its associated surface cold front seen as a region of strong temperature gradients within the dashed box in Figure 6(a). At lower values of shear, on the other hand, the upper-level trough broadens (Figure 6(d)) and continues to propagate eastward. Initially the cold fronts in both simulations were located at the same longitude, however as the simulations progressed the cyclonic behaviour cold front propagated eastward from its initial position whereas the anticyclonic behaviour cold front became stationary. This is precisely the change in cold front behaviour that is observed during SACZ onset as indicated by changes in the propagation and structure of cold front rainfall (Figures 3 and 4). It is suggested here that at the time when the SACZ becomes established, a regime change occurs whereby the horizontal shear of the environment becomes more anticyclonic, favouring the occurrence of midlatitude waves that have an anticyclonic or 'thinning trough' behaviour (as in Figure 6(b)), and giving rise to a stationary front ahead of the thinned upper-level trough (Figures 4 and 6(a)).

Further support for this hypothesis is shown in the daily sequences of GPCP rainfall and PV on the 320 K θ surface for the pre-onset and onset cold front events of 2003 shown in Figures 7 and 8. As it slopes downward from the Poles to the Tropics, the 320 K θ surface crosses the tropopause in midlatitudes reaching the mid-troposphere in the Subtropics. This means that in midlatitudes the 320 K θ surface PV can be thought of as representative of the upper-tropospheric flow. The 2003 pre-onset cold front daily plots shown in Figure 7 span the period from 27 October (day 0) to 30 October (day +3). The 320 K PV for the pre-onset cold front event shows an upper-level midlatitude trough that broadens (Figure 7(c)) and tilts cyclonically (Figure 7(d)) as it continues to propagate eastward past South America in a way that is reminiscent of the evolution in the 'cyclonic' shear simulation of Thorncroft *et al.* (1993) shown in Figure 6(d). The 2003 onset cold front daily plots shown in Figure 8 span the period from 1 November (day 0) to 4 November (day +3). The 320 K PV for the onset cold front event shows a very different evolution. In this case the upper-level midlatitude trough tilts anticyclonically (Figure 8(a)–(c)) as it propagates eastward past South America finally leaving a cut-off low behind (Figure 8(d)), in an evolution that is very similar to the 'anticyclonic shear' simulation of Thorncroft *et al.* (1993) shown in Figure 6(b). The evolution of the rainfall patterns in the 2003 pre-onset (Figure 7) and onset (Figure 8) cold front events resemble the composite patterns in Figures 3 and 4 in the sense that rainfall becomes stationary over the SACZ during the onset cold front, but not during the pre-onset cold front. The differences in evolution of the 2003 pre-onset and onset cold front events lend support to the hypothesis that monsoon onset in the SACZ is brought about by a regime change from midlatitude waves that have a 'broadening trough' behaviour prior to onset to midlatitude waves that have a 'thinning trough' behaviour at onset.

Figure 9 shows vertical cross-sections of the climatological zonal winds averaged over the longitudinal span of South America (30°W to 70°W). From October to December the midlatitude upper-level jet weakens somewhat as it migrates poleward from 30°S to 40°S. The climatological meridional shear of the mean zonal wind averaged between 30°W and 70°W is also shown in Figure 9. As the jet migrates poleward, anticyclonic shear becomes stronger in the latitudinal band where baroclinic systems that affect South America propagate (20°S to 40°S). The change in upper-level shear as the monsoon season progresses is likely caused, at least in part, by diabatic heating from Amazon convection through the establishment of the upper-level Bolivian high (e.g. Silva Dias *et al.*, 1983). The fact that onset in the SACZ region usually follows onset in the Amazon basin by a couple of pentads suggests that the effect of Amazon basin convection on the upper-level meridional wind shear may be necessary to help achieve the critical shear level that allows the

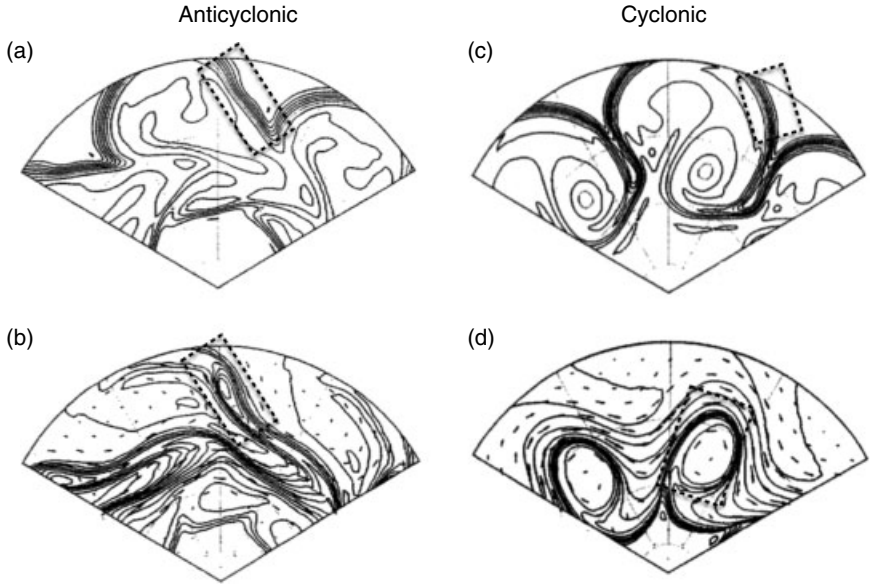

Figure 6. 'Anticyclonic' and 'cyclonic' behaviour midlatitude wave simulations from Thorncroft *et al.* (1993), adapted here to the Southern Hemisphere. (a, c) temperature at $\sigma = 0.967$ (near the surface), with contour interval 4 K, and (b, d) potential temperature on the -2 PVU surface (near the tropopause, 1 PVU $= 10^{-6}$ s^{-1} K kg^{-1}), with contour interval 5 K from 280 K. Lines of latitude and longitude are drawn every 20° and 30°, respectively. The dashed boxes in (a) and (c) mark the location of the surface cold front, and the dashed boxes in (b) and (d) mark the location of the upper-level trough.

transition from cyclonic to anticyclonic midlatitude wave behaviour.

Given the gradual nature of the change in shear, the question remains as to what would cause an abrupt change in midlatitude wave regime. Hartmann and Zuercher (1998) used numerical simulations of the lifecycles of midlatitude baroclinic waves to show that, when the barotropic shear crosses a critical threshold, an abrupt transition in midlatitude wave regime from cyclonic (as in Figures 3, 6(c) and (d), and 7) to anticyclonic (Figures 4, 6(a) and (b) and 8) behaviour. Our hypothesis is therefore that as the meridional shear on the equatorward side of the upper-level jet becomes gradually more anticyclonic, it suddenly crosses the critical threshold of horizontal shear needed to produce a sudden transition from a cyclonic to an anticyclonic or 'thinning trough' midlatitude baroclinic wave regime. When the meridional shear threshold is reached, the character of the frontal systems that pass through South America changes, ultimately causing the establishment of the SACZ and onset of the monsoon in southeastern Brazil. Although the observations shown here offer evidence that supports this hypothesis, further observational and modelling work that are beyond the scope of this study are required to prove it.

6. Conclusions

A hallmark feature of the South American monsoon system, the SACZ is easily seen in monthly mean summertime fields of rainfall in South America as a northwest–southeast band of rainfall that extends from the western part of the Amazon basin through southeastern Brazil and into the Atlantic Ocean. The SACZ lasts on average from about late October around (pentad 61; 28 October–1 November) to the following April (pentad 21; 11–15April). In contrast to the slow progression of monsoon onset over the Amazon basin, monsoon onset in the SACZ region is quite abrupt (NR10). This abrupt nature of monsoon onset in the SACZ onset suggests the presence of a fast dynamic trigger. The main objective of this study was to analyse the role of abrupt changes in the structure and propagation of cold fronts in the onset of the monsoon season in the SACZ region.

An REOF analysis of the 1979–2008 GPCP rainfall data was used to calculate monsoon onset dates in the SACZ region for each year of that 30-year period. The NCEP reanalysis SLP was then used to determine the dates when cold fronts passed through a base region located in subtropical South America. For each year, the last cold front that occurred before monsoon onset in the SACZ was labeled 'pre-onset', the cold front that occurred during the onset pentad was labeled 'onset' and the first cold front after onset was labelled 'post-onset'. Composites of the pre-onset, onset, and post-onset cold fronts were then produced using the GPCP rainfall and NCEP reanalysis datasets. While post-onset and onset composites were very similar, the composites of pre-onset and onset cold fronts showcased dramatic changes in the structure and propagation of cold fronts at the time of monsoon onset in the SACZ.

Pre-onset and onset composites were similar during the early stages of the cold front passage over South America. For example, it is clear from these composites that at the time of monsoon onset in the SACZ, not only was rainfall already present in the western two-thirds of the Amazon basin, but also the Bolivian high, another hallmark feature of the mature monsoon in the Amazon basin, was already present in the 200 mb streamlines (not shown) prior to monsoon onset in the SACZ region. This further confirms the observation that monsoon onset in most of the Amazon basin precedes monsoon onset in the SACZ region.

However, after the cold front passes through the base region on day 0, pre-onset and onset composites become very different. While pre-onset cold fronts weaken, become disconnected from the Amazon basin rainfall and propagate

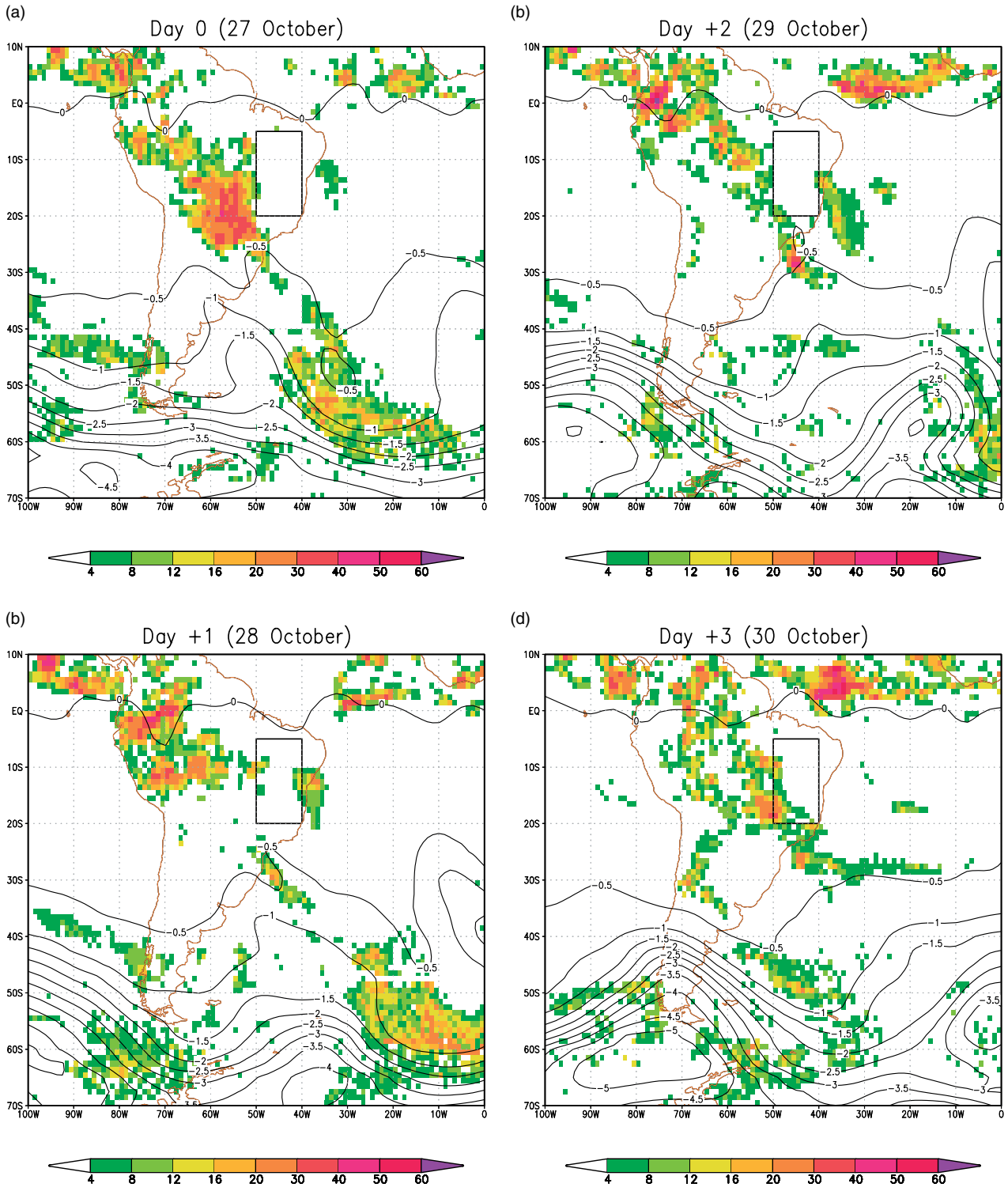

Figure 7. Potential vorticity on the 320 K potential temperature surface (contours, PVU) and GPCP rainfall (shading, mm day^{-1}) for the 2003 'pre-onset' cold front event. The solid box indicates the SACZ region. This figure is available in colour online at wileyonlinelibrary.com/journal/qj

into the South Atlantic Ocean without ever reaching the SACZ region, onset cold fronts continue to propagate northeastward along the South American coast, becoming stationary along the SACZ region for a few days. During this time the onset cold fronts are shaped as northwest-to-southeast elongated regions of rainfall that extend from the western Amazon basin into the South Atlantic Ocean. This abrupt change in the structure and propagation of frontal systems as they pass through South America suggests that the abrupt onset of the monsoon in the SACZ occurs at the time when the first cold front of the monsoon season becomes stationary along the southeastern coast of Brazil. Analysis of composites of 200 mb geopotential anomalies as well as a case-study of daily 320 K PV showed that the midlatitude baroclinic cyclones associated with the onset cold fronts behave very differently from those associated with the pre-onset cold fronts. In particular, onset cold fronts are associated with midlatitude cyclones which appear to follow a 'thinning trough' or 'anticyclonic' baroclinic wave life cycle that has been shown to favour the

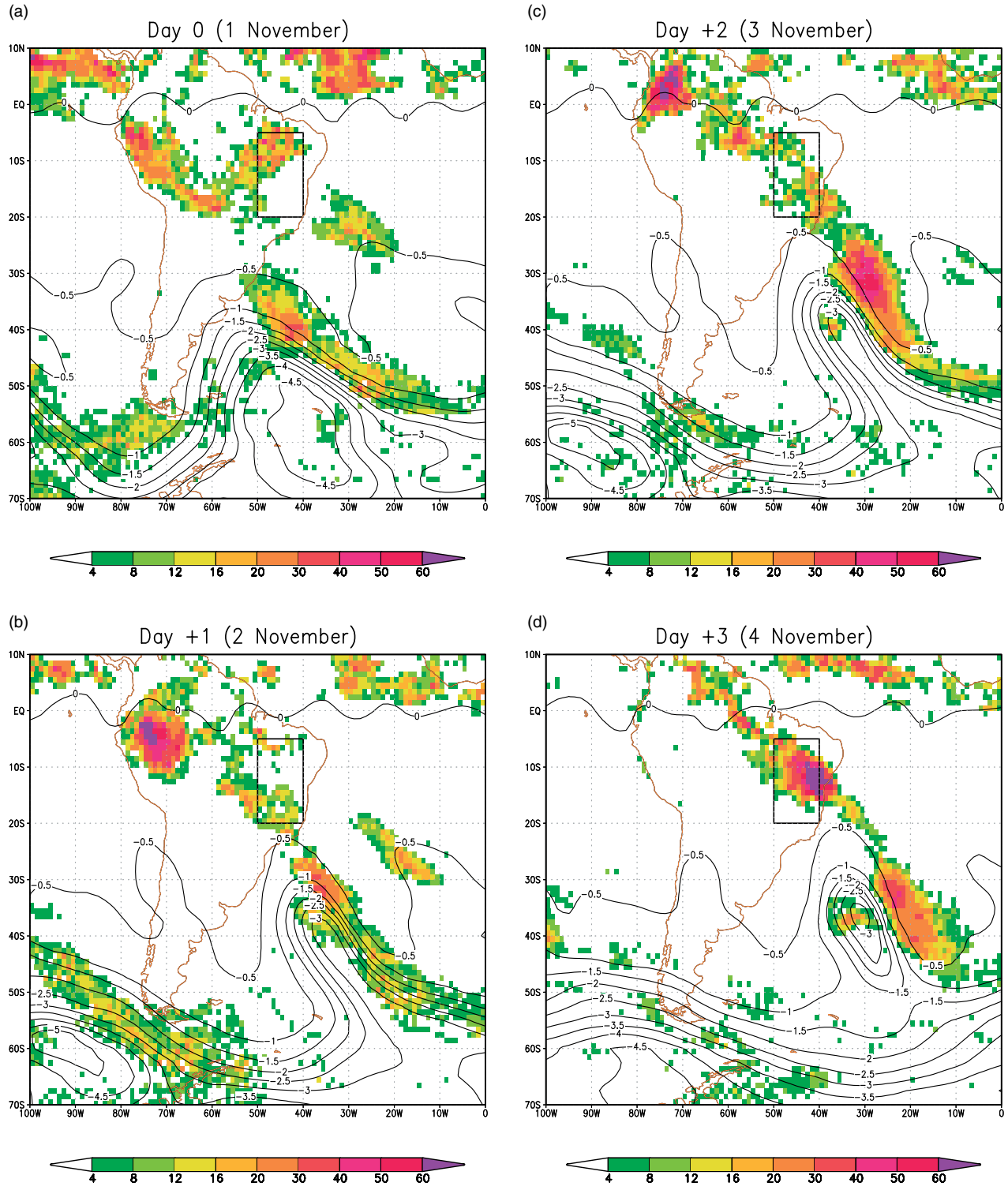

Figure 8. As Figure 7, but for the 2003 'onset' cold front event. This figure is available in colour online at wileyonlinelibrary.com/journal/qj

presence of stationary cold fronts. This observation suggests that an abrupt change in the life cycles of midlatitude baroclinic waves travelling across South America is a possible mechanism for the abrupt changes in cold front behaviour observed at the time of onset of the monsoon season in the SACZ region.

In summary, this study shows that the abrupt onset of the monsoon in the SACZ is due to an abrupt change in the structure and propagation of frontal systems as they pass through South America with cold fronts suddenly becoming stationary along the southeastern coast of Brazil and organizing a band of convection that stretches from the Atlantic Ocean to the Amazon basin. This study also offers evidence for a mechanism to explain this abrupt change in the structure and propagation of cold fronts across South America via a sudden transition from a 'cyclonic' or 'broadening trough' to an 'anticyclonic' or 'thinning trough' midlatitude baroclinic wave regime. Further observational and modelling studies of the onset of the monsoon in the SACZ region are under way to validate this hypothesized mechanism.

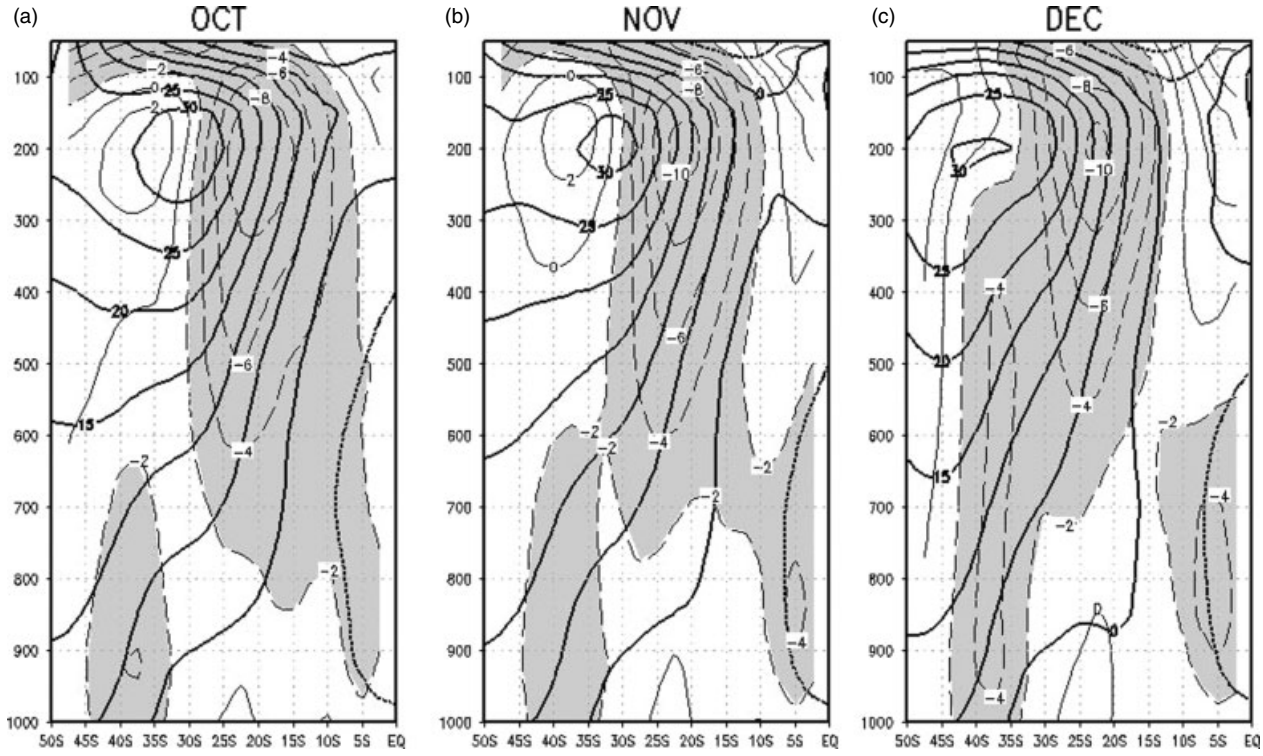

Figure 9. October–December vertical cross-sections of the climatological zonal wind averaged between 70°W and 30°W (bold contours, m s^{-1}) and north–south wind shear (thin contours, m s^{-1} per 2.5 degrees of latitude). Shading indicates anticyclonic shear.

Acknowledgements

This study has been funded by a grant (award number NA07OAR4310495) from the National Oceanic and Atmospheric Administration Climate and Global Change Program Climate Prediction Program for the Americas (NOAA-CPPA). We also thank three anonymous reviewers for their invaluable comments.

References

Adler RF, Huffman GJ, Chang A, Ferraro R, Xie P-P, Janowiak J, Rudolf B, Schneider U, Curtis S, Bolvin D, Gruber A, Susskind J, Arkin P, Nelkin E. 2003. The version-2 Global Precipitation Climatology Project (GPCP) monthly precipitation analysis (1979–present). *J. Hydrometeorol.* **4**: 1147–1167.

Chang CP, Chen GTJ. 1995. Tropical circulation associated with southwest monsoon onset and westerly surges over the South China Sea. *Mon. Weather Rev.* **123**: 181–196.

Davies HC, Schär C, Wernli H. 1991. The palette of fronts and cyclones within a baroclinic wave development. *J. Atmos. Sci.* **48**: 1666–1689.

Fortune M, Kousky V. 1983. Two severe freezes in Brazil: Precursors and synoptic evolution. *Mon. Weather Rev.* **111**: 181–196.

Fu R, Li W. 2004. The influence of the land surface on the transition from dry to wet season in Amazonia. *Theor. Appl. Climatol.* **78**: 97–110.

Gan MA, Rao VB. 1984. The influence of the Andes Cordillera on transient disturbances. *Mon. Weather Rev.* **122**: 1141–1157.

Garreaud RD. 2000. Cold air intrusions over subtropical South America: Structure and dynamics. *Mon. Weather Rev.* **128**: 2544–2599.

Gonzalez M, Vera C, Liebmann B, Marengo J, Kousky V, Allured D. 2007. The nature of the rainfall onset over central South America. *Atmósfera* **20**: 379–396.

Hartmann DL, Zuercher P. 1998. Response of baroclinic life cycles to barotropic shear. *J. Atmos. Sci.* **55**: 297–313.

Horel JD, Hahmann AN, Geisler JE. 1989. An investigation of the annual cycle of convective activity over the tropical Americas. *J. Climate* **2**: 1388–1403.

Hoskins BJ, West NV. 1979. Baroclinic waves and frontogenesis. Part II: uniform potential vorticity jet flows – cold and warm fronts. *J. Atmos. Sci.* **36**: 1663–1680.

Huffman GJ, Adler RF, Morrissey M, Bolvin DT, Curtis S, Joyce R, McGavock B, Susskind J. 2001. Global precipitation at one-degree daily resolution from multi-satellite observations. *J. Hydrometeorol.* **2**: 36–50.

Kalnay E, Kanamitsu M, Kistler R, Collins W, Deaven D, Gandin L, Iredell M, Saha S, White G, Woollen J, Zhu Y, Chelliah M, Ebisuzaki W, Higgins W, Janowiak J, Mo KC, Ropelewski C, Wang J, Leetma A, Reynolds R, Jenne R, Joseph D. 1996. The NCEP/NCAR 40-year reanalysis project. *Bull. Amer. Meteorol. Soc.* **77**: 437–472.

Kousky VE. 1988. Pentad outgoing longwave radiation climatology for the South American sector. *Rev. Bras. Meteorol.* **3**: 217–231.

Kousky VE, Gan MA. 1981. Upper tropospheric cyclonic vortices in the tropical South Atlantic. *Tellus* **33**: 538–551.

Li W, Fu R. 2004. Transition of the large-scale atmospheric and land surface conditions from the dry to the wet season over Amazonia as diagnosed by the ECMWF re-analysis. *J. Climate* **17**: 2637–2651.

Li W, Fu R. 2006. Influence of cold air intrusions on the wet season onset over Amazonia. *J. Climate* **19**: 257–275.

Liebmann B, Marengo JA. 2001. Interannual variability of the rainy season and rainfall in the Brazilian Amazon Basin. *J. Climate* **14**: 4308–4318.

Liebmann B, Kiladis GN, Marengo JA, Ambrizzi T, Glick JD. 1999. Submonthly convective variability over South America and the South Atlantic Convergence zone. *J. Climate* **12**: 1877–1891.

Lupo AR, Nocera J, Bosart LF, Hoffman EG, Knight DJ. 2001. South American cold surges: types, composites, and case studies. *Mon. Weather Rev.* **129**: 1021–1041.

Marengo JA, Liebmann B, Kousky VE, Filizola NP, Wainer IC. 2001. Onset and end of the rainy season in the Brazilian Amazon basin. *J. Climate* **14**: 833–852.

Marengo JAC, Satyamurty P, Nobre C, Sea W. 1997. Cold surges in tropical and extratropical South America: the strong event in June 1994. *Mon. Weather Rev.* **125**: 2759–2786.

Mendes MCD, Trigo RM, Cavalcanti IFA, DaCamara CC. 2008. Blocking episodes in the Southern Hemisphere: impact on the climate of adjacent continental areas. *Pure Appl. Geophys.* **165**: 1941–1962. DOI: 10.1007/s00024-008-0409-4.

Nieto-Ferreira R, Rickenbach TM. 2011. Regionality of monsoon onset in South America: A three-stage conceptual model. *Internat. J. Climatol.* **31**: DOI: 10.1002/joc.2161.

Nieto-Ferreira R, Rickenbach TM, Herdies DL, Carvalho LMV. 2003. Variability of South American convective cloud systems and tropospheric circulation during January–March 1998 and 1999. *Mon. Weather Rev.* **131**: 961–973.

Nogues-Paegle JN, Mo KC. 1997. Alternating wet and dry conditions over South America during summer. *Mon. Weather Rev.* **125**: 279–291.
North GR, Bell TL, Cahalan RF, Moeng FJ. 1982. Sampling errors in the estimation of empirical orthogonal functions. *Mon. Weather Rev.* **110**: 699–706.
Raia A, Cavalcanti IFA. 2008. The life cycle of the South American monsoon system. *J. Climate* **21**: 6227–6246.
Rickenbach TM, Nieto Ferreira R, Halverson J, Herdies DL, Silva Dias MAF. 2002. Modulation of convection in the southwestern Amazon basin by extratropical stationary fronts. *J. Geophys. Res.* **107**: 8040, DOI: 10.1029/2000JD000263.
Shapiro MA, Wernli H, Bond NA, Langland R. 2001. The influence of the 1997–1999 El Niño Southern Oscillation on extratropical baroclinic life cycles over the eastern North Pacific. *Q. J. R. Meteorol. Soc.* **127**: 331–342.
Silva VBS, Kousky VE. 2001. Intraseasonal precipitation over eastern Brazil during the summer of 1991–2000 (in Portuguese). *Rev. Bras. Meteorol.* **16**: 187–199.
Silva Dias PL, Schubert WH, DeMaria M. 1983. Large-scale response of the tropical atmosphere to transient convection. *J. Atmos. Sci.* **40**: 2689–2707.
Thorncroft CD, Hoskins BJ, McIntyre ME. 1993. Two paradigms of baroclinic wave life-cycle behaviour. *Q. J. R. Meteorol. Soc.* **119**: 17–55.
Velasco I, Fritsch JM. 1987. Mesoscale convective complexes in the Americas. *J. Geophys. Res.* **92**: 9591–9613.
Vera CS, Vigliarolo PK. 2000. A diagnostic study of cold-air outbreaks over South America. *Mon. Weather Rev.* **128**: 3–24.
Zhou J, Lau KM. 1998. Does a monsoon climate exist over South America? *J. Climate* **11**: 1020–1040.

